

One-pot Synthesis of Trifunctional Epoxy Resin and its Nanocomposite: Investigation of Thermal and Rheological Properties

Naoual El-Aouni ¹, Rachid Hsissou ^{1,2,*} , Jalila El Azzaoui ¹, Mehdi El Bouchti ³, Abderrahim Elbachiri ⁴, Ahmed Elharfi ⁵, Mohamed Rafik ¹

¹ Laboratory of Organic and Inorganic Chemistry, Electrochemistry and Environment, Department of Chemistry, Faculty of Sciences, University Ibn Tofail, BP 242, 14000, Kenitra, Morocco

² Team of Innovative Materials and Mechanical Manufacturing Processes, ENSAM, Moulay Ismail University, B.P. 15290, Al Mansour, Meknes, Morocco

³ Laboratory REMTEX, ESITH (Hight School of Textile and Clothing Industries), Casablanca, Morocco

⁴ Royal Naval School, University Department - Boulevard Sour- Jdid, Casablanca, Morocco

⁵ Laboratory of Advanced Materials and Process Engineering, Department of Chemistry, Faculty of Sciences, University Ibn Tofail, BP 242, 14000, Kenitra, Morocco

* Correspondence: r.hsissou@gmail.com;

Scopus Author ID 57193233249

Received: 2.12.2020; Revised: 28.12.2020; Accepted: 2.01.2021; Published: 4.01.2021

Abstract: Herein, in the present study, we developed the synthesis of new trifunctional epoxy resin (TER) namely triglycidyl ether N,N bis (3-phenylamino propyl) 3-phenylamino propoxy phenyl and the elaboration of its nanocomposite. TER was characterized and confirmed using Fourier transform infrared and nuclear magnetic resonance spectroscopy. Further, the storage modulus and loss modulus for all formulated nanocomposite increase with the increase in the zinc oxide filler. The results of the thermogravimetric analysis confirm the amelioration in the thermal properties of different nanocomposites TER/MDA/ZnO crosslinked by methylene dianiline (MDA) and formulated by zinc oxide (ZnO) as a filler at varying mass percentage (0, 0.5, 1, and 2%).

Keywords: synthesis; epoxy resin; nanocomposite; rheological; thermogravimetric analysis.

© 2020 by the authors. This article is an open-access article distributed under the terms and conditions of the Creative Commons Attribution (CC BY) license (<https://creativecommons.org/licenses/by/4.0/>).

1. Introduction

Epoxy resins are widely used and employed in several industrial application fields such as aerospace, automotive, encapsulate electrical and electronic components [1-4]. Epoxy resins thermosetting are the most commonly used owing to their excellent thermal and mechanical properties and their exceptional anticorrosive coatings properties [5-10]. However, some current problems in the thermosetting resins applications are low stiffness and strength, as well as exothermic heat generated by the curing of epoxy resins. Then, additives are often employed to modify materials' characteristics and properties, including diluents, loads, modifiers, flame retardants, antioxidants, or plasticizers [11-17]. Several researchers have currently adopted that the addition of zinc oxide compound in the epoxy resin matrix exhibits high flame retardancy and thermal stability [18-22]. Further, liquid crystal epoxy resins are widely investigated because of their unusual mechanical and thermal properties, little shrinkage in curing, low thermal expansion coefficient, and dielectric constant [23-27]. The advanced applications of epoxy resins are not alone very demanding, but many new applications with new performance

requirements are developed every year [28-32]. In addition, the rheological properties of epoxy resins and their nanocomposites are very interesting. The incorporation of zinc oxide as a charge in elaborated nanocomposites could be increasing the storage modulus and the loss modulus. Also, the increase of storage modulus and the loss modulus depends on the dispersion of filler addition into formulated nanocomposite [33-38]. In this potential study, we synthesized and developed the triglycidyl ether N,N bis (3-phenylamino propyl) 3-phenylamino propoxy phenyl trifunctional epoxy resin was identified and confirmed using FTIR and NMR spectroscopy. Moreover, viscosity, rheological, and thermal analyses of the TER and its nanocomposite were examined using an Ubbelohd VB-1423 capillary viscosimeter, RHM01-RD HAAKE rheometer, and thermogravimetric analysis, respectively.

2. Materials and Methods

2.1. Synthesis of trifunctional epoxy resin (TER).

Triglycidyl of para aminophenol (TGPAP), aniline (98%), epichlorohydrin (99%), triethylamine (97%), methylene dianiline (99%), zinc oxide, and methanol were purchased by Aldrich Chemical Company and used without any other purification. Trifunctional epoxy resin, namely triglycidyl ether N,N bis (3-phenylamino propyl) 3-phenylamino propoxy phenyl (TER) was synthesis in two steps according to the procedure reported in many works of literature [39-41]. In the first step, 5.5×10^{-3} mol of aniline as the nucleophilic group was added to 6.54×10^{-3} mol of TGPAP with magnetic stirring for 6 h at 80 °C to open the epoxy groups. During the second step, 5.53×10^{-3} mol of epichlorohydrin was added to the intermediate product by condensation reaction with magnetic stirring for 4 h at 70 °C. Besides, 9.85×10^{-3} mol of triethylamine as a basis was added to the reaction mixture with magnetic stirring for 3 h at 40 °C. TER epoxy resin was obtained by removing the secondary products using the rotary evaporator. Finally, TER was obtained with a yield of 92 % (Figure 1).

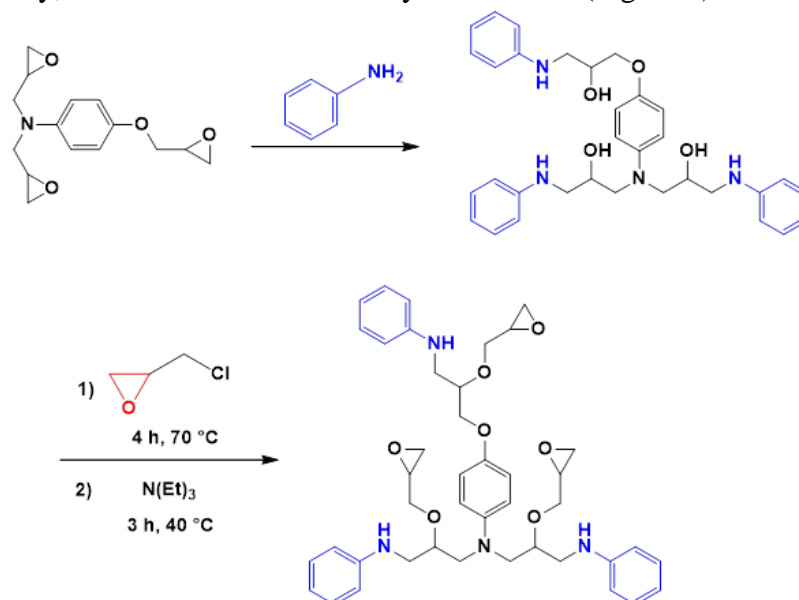


Figure 1. Synthesis of trifunctional epoxy resin (TER).

2.2. Curing of trifunctional epoxy resin (TER).

TER was cured using methylene dianiline (MDA) as a curing agent to form a three-dimensional material (Figure 2). Then, the four hydrogens atoms of methylene dianiline react

with the oxirane groups of TER by the condensation reaction. Besides, MDA and TER are curing in the oven at 80 °C. Moreover, TER was mixed with MDA to provide a single-phase [42, 43]. Further, the development specimens were placed in a geometrically designed mold at 70°C for 24 h. Finally, we proceeded to develop the nanocomposite using the identical procedure above in the hardening of TER with MDA and zinc oxide (ZnO) as charge at different percentages (0, 0.5, 1, and 2%) [20].

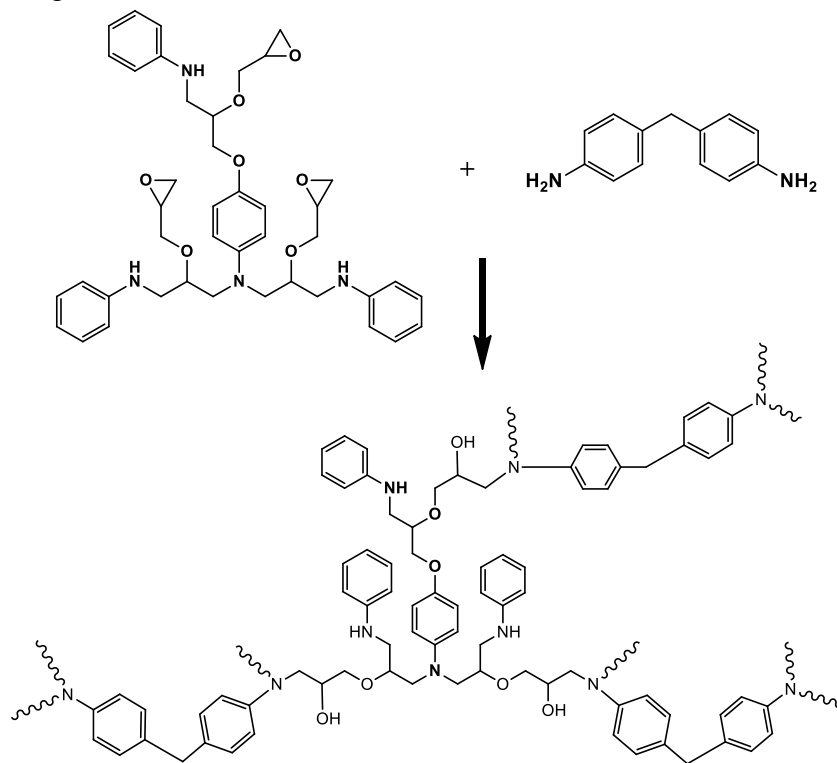


Figure 2. TER crosslinking using MDA.

2.3. Fourier-transform infrared spectroscopy.

The infrared spectrometer used is BRUKER Fourier transformed infrared spectrometer (FTIR). The light beam passes through the specimen to a thickness of about 2 μm . The analysis is carried out between 4000 cm^{-1} and 600 cm^{-1} .

2.4. Nuclear magnetic resonance.

The nuclear magnetic resonance (^1H NMR and ^{13}C NMR) analysis was obtained using an apparatus of Bruker AVANCE 300 by dissolving the product in DMSO. The chemical displacements are presented in ppm. The letter s, d, t, q, and m denote singlet, doublet, triplet, quadruplet, and multiplet, respectively.

2.5. Rheological analysis.

The viscosimetric and rheological properties of epoxy resin and its composites were analyzed using capillary viscosimeter VB-1423 of the Ubbelohd and RHM01-RD HAAKE rheometer (HAAKE MARS), respectively.

2.6. Thermogravimetric analysis.

To realize our study, which deals with the degradation of elaborated epoxy resin and its nanocomposites, we employed the thermogravimetric analysis method (ATG). Measurements

of the kinetics of degradation by mass loss were carried by using a SETARAM TAG 24S. The heating rate is 10 °C/min, and the range of the measurement temperature is 0 to 600 °C.

3. Results and Discussion

3.1. FTIR and NMR characterization.

Fourier transform infrared (FTIR) and nuclear magnetic resonance (^1H NMR and ^{13}C NMR) analyses were realized to confirm the chemical structure of the triglycidyl ether N,N bis (3-phenylamino propyl) 3-phenylamino propoxy phenyltrifunctional epoxy resin. FTIR, ^1H NMR, and ^{13}C NMR spectrums of TER are displayed in Figures 3, 4, and 5. Then, the different bands and chemical shift results obtained of the trifunctional epoxy resin are reported below.

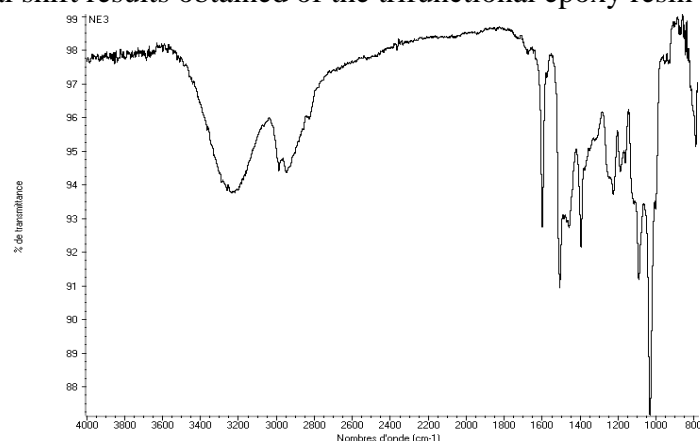


Figure 3. IR spectra of TER.

FTIR (cm⁻¹): 3240 (band of N-H), 2900 (band of CH₂ linked to oxygen), 1450-1580 (band of N-C linked to aromatic rings), 1400 (band of C-N-Ar), 1030 (band of aromatic C-H), and 820 (band of oxirane group).

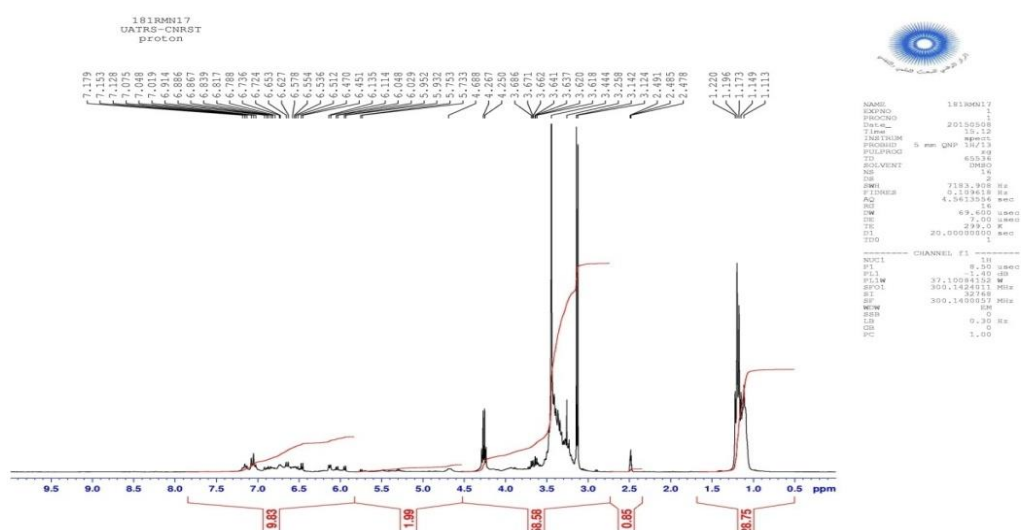


Figure 4. ^1H NMR spectra of TER.

^1H NMR (ppm): 1.2 (solvent); 2.5 (d, 6H, CH₂ of oxirane group); 3 (m, 3H, CH of oxirane group); 3.3 (m, 3 H, CH linked to CH aliphatic); 3.5 (d, 6H, CH₂ linked to oxirane group and nitrogen); 3.7 (d, 6 H, CH₂ linked to phenylamino); 4.3 (s, 3 H, NH linked to phenyl); 6-6.3 (m, 15 H, CH aromatic), 6.6 (d, 2 H, CH aromatic of N in ortho position), and 7.2 (d, 2 H, CH aromatic of N in meta position).



3.2. Viscosity study.

Temperature (°C)	5% Viscosity (mm²/s)	10% Viscosity (mm²/s)	15% Viscosity (mm²/s)	20% Viscosity (mm²/s)
30	0.97	1.11	1.23	1.38
35	0.95	1.08	1.19	1.34
40	0.93	1.05	1.16	1.32
45	0.91	1.02	1.14	1.30
50	0.89	1.00	1.12	1.28
55	0.87	0.97	1.10	1.25

The viscosity of the (TER/Ethanol) system increases with the increase in the weight percentage of trifunctional epoxy resin at each temperature. This augmentation can be explained by the increase in the molecular mass of the (TER/Ethanol) system [44-46]. This due to the increase in the (TER/Ethanol) system's density by a strong interaction between the bonds

of the epoxy resin employed. As the temperature increase suggests, the viscosity of (TER/Ethanol) system is decreasing. This decrease in viscosity indicates that the density is becoming low. Therefore, the heat is given by the apparatus feebleness the interaction between the bonds of TER. Further, the viscosity changes from a viscous state to a liquid state.

3.3. Rheological properties.

Rheological properties are interesting properties that affect the processing of the formulation of the nanocomposite. Variation of storage modulus G' and loss modulus G'' versus frequency for nanocomposite pure (TER/MDA) and formulated nanocomposites (TER/MDA/ZnO) with various percentages of zinc oxide are plotted in Figure 7 and 8.

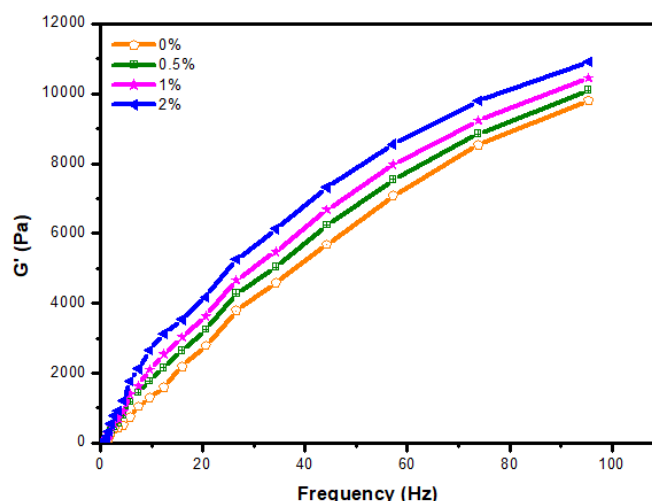


Figure 7. Storage modulus G' for TER/MDA/ZnO according to frequency.

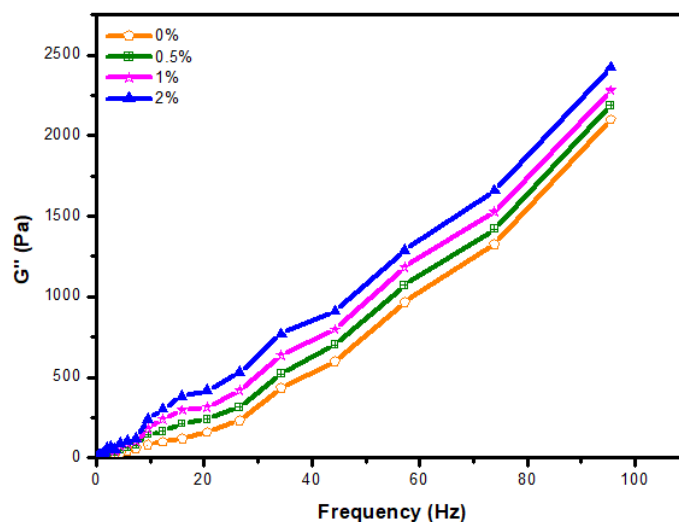


Figure 8. Loss modulus G'' for TER/MDA/ZnO according to frequency.

Storage modulus G' and loss modulus G'' values of different nanocomposites increase with increasing zinc oxide as charge [47, 48]. The loss modulus G'' was significantly lower than the storage modulus G' over the entire frequency examined for nanocomposite crosslinked by methylene dianiline and formulated with different zinc oxide percentages. The storage modulus G' of all prepared nanocomposite increases with an increase in ZnO percentages [40, 49]. This result indicates the progressive curing of the three-dimensional network. The rheological behaviors were highly correlated with the formulation of the nanocomposites.

3.4. Thermal properties.

The thermal properties of the TER crosslinked by methylene dianiline as a hardener and formulated with zinc oxide (ZnO) as a filler (TER/MDA/ZnO) at various percentages were measured by thermogravimetric analysis (TGA). The TGA plots are displayed in Figure 9. The TGA results are depicted in Table 1 (T_d , T_{50} and R (500 °C)). The temperature at which decomposition begins, decomposition temperature at 50% of weight loss, and the residual amount at 500 °C, respectively). The result in Table 1 indicates that the residual amount of the formulated nanocomposite (TER/MDA/ZnO) is a higher value compared with the TER/MDA pure [50-54]. The reason is that zinc oxide does not decompose below 500 °C. Further, the higher the zinc oxide's mass ratio in the nanocomposite (TER/MDA/ZnO) elevates, the residual amount elevates consequently. All TGA plots display one peak, indicating thermal degradation of the elaborated nanocomposites [55-57]. Then, the temperature peak of the nanocomposite pure (TER/MDA) is 220 °C. The weight loss of the (TER/MDA) begins from 220 °C and loses all its weight at 409 °C. However, the temperature peak of the formulated nanocomposite (TER/MDA/ZnO) is 268 °C. The weight loss of the (TER/MDA/ZnO) starts from 268 °C and loses all its weight at 477 °C. Also, the temperature peak of the formulated nanocomposite (TER/MDA/ZnO) is higher than that of nanocomposite pure (TER/MDA) [20, 58, 59].

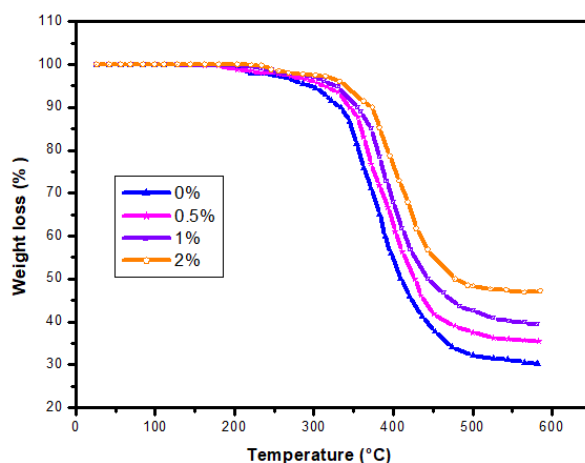


Figure 9. TGA plots of TER/MDA and TER/MDA/ZnO.

Table 1. TGA data of TER/MDA and TER/MDA/ZnO.

Nanocomposites	T_d (°C)	T_{10} (°C)	T_{50} (°C)	S_{dr} (°C)	R (%) (500 °C)
TER/MDA/0% ZnO	220	333	409	344	32.5
TER/MDA/0.5% ZnO	235	345	427	356	37.6
TER/MDA/1% ZnO	255	357	443	368	42.5
TER/MDA/2% ZnO	268	374	477	381	48.5

4. Conclusions

In this study, we have developed and investigated the triglycidyl ether N,N bis (3-phenylamino propyl) 3-phenylamino propoxy phenyl (TER) trifunctional epoxy resin. Epoxy resin (TER) was identified using FTIR and NMR spectroscopy. Viscosimetric behaviors of TER/Ethanol decreased with an increase in temperature. Further, TER/MDA/ZnO curing by methylene dianiline and formulated by zinc oxide were investigated as potential nanocomposite for rheological and thermogravimetric analysis. Then, storage modulus and the loss modulus for varying nanocomposites elevate with both the elevate into zinc oxide and frequency. This could explain that the charge employed incorporated into nanocomposites is very well

formulated. The thermogravimetric analysis data confirm the amelioration of the thermal properties of varying nanocomposites formulated at different percentages of ZnO.

Funding

This research received no external funding.

Acknowledgments

Many thanks to Prof. Ahmed ELHARFI at University IbnTofail, Morocco. Many thanks to Doctor Rachid HSISSOU, who collaborated to the success of this paper. All evaluators of this work gave enough time to review it with their excellent remarks and questions to give it some value.

Conflicts of Interest

The authors declare no conflict of interest.

References

1. Yao, W.; Zhang, Q.; Qi, F.; Zhang, J.; Liu, K.; Li, J.; Chen, W.; Du, Y.; Jin, Y.; Liang, Y.; Liu, N. Epoxy containing solid polymer electrolyte for lithium ion battery. *Electrochim. Acta* **2019**, *318*, 302-313, <https://doi.org/10.1016/j.electacta.2019.06.069>.
2. Ou, B.; Chen, M.; Guo, Y.; Kang, Y.; Guo, Y.; Zhang, S.; Yan, J.; Liu, Q.; Li, D. Preparation of novel marine antifouling polyurethane coating materials. *Polym. Bull.* **2018**, *75*, 5143-5162, <https://doi.org/10.1007/s00289-018-2302-5>.
3. Liang, Y.; Liu, B.; Zhang, B.; Liu, Z.; Liu, W. Effects and mechanism of filler surface coating strategy on thermal conductivity of composites: A case study on epoxy/SiO₂-coated BN composites. *Int. J. Heat Mass Transfer* **2021**, *164*, 120533, <https://doi.org/10.1016/j.ijheatmasstransfer.2020.120533>.
4. Lin, T.A.; Lin, J.-H.; Bao, L. A study of reusability assessment and thermal behaviors for thermoplastic composite materials after melting process: Polypropylene/ thermoplastic polyurethane blends. *Journal of Cleaner Production* **2021**, *279*, 123473, <https://doi.org/10.1016/j.jclepro.2020.123473>.
5. Zoukrami, F.; Haddaoui, N.; Sclavons, M.; Devaux, J.; Vanzeveren, C. Rheological properties and thermal stability of compatibilized polypropylene/untreated silica composites prepared by water injection extrusion process. *Polym. Bull.* **2018**, *75*, 5551-5566, <https://doi.org/10.1007/s00289-018-2344-8>.
6. Hsissou, R.; Benhiba, F.; Dagdag, O.; El Bouchti, M.; Nouneh, K.; Assouag, M.; Briche, S.; Zarrouk, A.; Elharfi, A. Development and potential performance of prepolymer in corrosion inhibition for carbon steel in 1.0 M HCl: Outlooks from experimental and computational investigations. *J. Colloid Interface Sci.* **2020**.
7. Safaie, B.; Youssefi, M.; Rezaei, B. Rheological behavior of polypropylene/carbon quantum dot nanocomposites: the effects of particles size, particles/matrix interface adhesion, and particles loading. *Polym. Bull.* **2019**, *76*, 4335-4354, <https://doi.org/10.1007/s00289-018-2611-8>.
8. Dagdag, O.; Safi, Z.; Hsissou, R.; Erramli, H.; El Bouchti, M.; Wazzan, N.; Guo, L.; Verma, C.; Ebenso, E.E.; El Harfi, A. Epoxy pre-polymers as new and effective materials for corrosion inhibition of carbon steel in acidic medium: Computational and experimental studies. *Sci. Rep.* **2019**, *9*, 11715, <https://doi.org/10.1038/s41598-019-48284-0>.
9. Hsissou, R.; Bekhta, A.; Dagdag, O.; El Bachiri, A.; Rafik, M.; Elharfi, A. Rheological properties of composite polymers and hybrid nanocomposites. *Heliyon* **2020**, *6*, e04187, <https://doi.org/10.1016/j.heliyon.2020.e04187>.
10. Hsissou, R.; Benhiba, F.; About, S.; Dagdag, O.; Benkhaya, S.; Berisha, A.; Erramli, H.; Elharfi, A. Trifunctional epoxy polymer as corrosion inhibition material for carbon steel in 1.0 M HCl: MD simulations, DFT and complexation computations. *Inorg. Chem. Commun.* **2020**, *115*, 107858, <https://doi.org/10.1016/j.inoche.2020.107858>.
11. El Gouri, M.; El-Harfi, A. Modifications chimiques de l'hexachlorocyclotriphosphazène-Préparation de retardateurs de flame et de matériaux polymères ignifuges écologiques (Chemical modification of

- hexachlorocyclotriphosphazene-Preparation of flame retardants and ecological flame retardant polymers). *Journal of Materials and Environmental Science* **2012**, *3*, 17-33.
12. Li, S.; Yao, Y. Synergistic improvement of epoxy composites with multi-walled carbon nanotubes and hyperbranched polymers. *Composites Part B: Engineering* **2019**, *165*, 293-300, <https://doi.org/10.1016/j.compositesb.2018.11.122>.
 13. Zotti, A.; Zuppolini, S.; Borriello, A.; Zarrelli, M. The effect of glassy and rubbery hyperbranched polymers as modifiers in epoxy aeronautical systems. *Composites Part B: Engineering* **2019**, *169*, 88-95, <https://doi.org/10.1016/j.compositesb.2019.04.006>.
 14. Jia, S.; Wang, F.; Xu, B.; Yan, W. A developed energy-dependent model for studying thermal shock damage and phase transition of composite reinforced panel subjected to lightning strike. *European Journal of Mechanics - A/Solids* **2021**, *85*, 104141, <https://doi.org/10.1016/j.euromechsol.2020.104141>.
 15. Zhang, S.; Li, Z.; Guo, Y.; Cai, L.; Manikandan, P.; Zhao, K.; Li, Y.; Pol, V.G. Room-temperature, high-voltage solid-state lithium battery with composite solid polymer electrolyte with in-situ thermal safety study. *Chem. Eng. J.* **2020**, *400*, 125996, <https://doi.org/10.1016/j.cej.2020.125996>.
 16. Yin, H.; Gao, S.; Cai, Z.; Wang, H.; Dai, L.; Xu, Y.; Liu, J.; Li, H. Experimental and numerical study on thermal protection by silica aerogel based phase change composite. *Energy Reports* **2020**, *6*, 1788-1797, <https://doi.org/10.1016/j.egyr.2020.06.026>.
 17. Haoliang, T.; Changliang, W.; Mengqiu, G.; Yongjing, C.; Junguo, G.; Zhihui, T.; Yi, L.; Cong, S.; Hao, W.; Guo, J.; Shicheng, W. Study on process and performance of thermal protective coating on polyimide resin matrix composite. *Ceram. Int.* **2020**, *46*, 12744-12758, <https://doi.org/10.1016/j.ceramint.2020.02.043>.
 18. Hsissou, R.; Abbout, S.; Seghiri, R.; Rehioui, M.; Berisha, A.; Erramli, H.; Assouag, M.; Elharfi, A. Evaluation of corrosion inhibition performance of phosphorus polymer for carbon steel in [1 M] HCl: Computational studies (DFT, MC and MD simulations). *Journal of Materials Research and Technology* **2020**, *9*, 2691-2703, <https://doi.org/10.1016/j.jmrt.2020.01.002>.
 19. El-Aouni, N.; Benabida, A.; Cherkaoui, M.; Elharfi, A. A New Epoxy Resin Based Organic Molecule as an Effective Inhibitor of Mild Steel Corrosion in a Sulfuric Acid Medium. *Journal of Chemical Technology & Metallurgy* **2018**, *53*, 878-890.
 20. El-Aouni, N.; Hsissou, R.; Azzaoui, J.E.; Bouchti, M.E.; Elharfi, A. Synthesis rheological and thermal studies of epoxy polymer and its composite. *Chemical Data Collections* **2020**, *30*, 100584, <https://doi.org/10.1016/j.cdc.2020.100584>.
 21. Hsissou, R.; Benhiba, F.; Echihi, S.; Benkhaya, S.; Hilali, M.; Berisha, A.; Briche, S.; Zarrouk, A.; Nouneh, K.; Elharfi, A. New epoxy composite polymers as a potential anticorrosive coatings for carbon steel in 3.5% NaCl solution: Experimental and computational approaches. *Chemical Data Collections* **2021**, *31*, 100619, <https://doi.org/10.1016/j.cdc.2020.100619>.
 22. Zhang, L.F.; Gao, R.; Hou, J.; Zhao, B.L.; Sun, M.; Hao, T.; Xie, Z.M.; Liu, R.; Wang, X.P.; Fang, Q.F.; Liu, C.S. Study on thermal stability and irradiation response of copper/iron nano-multilayer composite fabricated by cross accumulative roll bonding. *J. Nucl. Mater.* **2021**, *543*, 152548, <https://doi.org/10.1016/j.jnucmat.2020.152548>.
 23. Cheng, K.-C.; Yu, S.-Y.; Chiu, W.-Y. Thermal properties of side-chain phosphorus-containing epoxide cured with amine. *J. Appl. Polym. Sci.* **2002**, *83*, 2741-2748, <https://doi.org/10.1002/app.10161>.
 24. Castell, P.; Serra, A.; Galià, M. Liquid-crystalline thermosets from liquid-crystalline epoxy resins containing bisazomethinebiphenylene mesogens in the central core: Copolymerization with a nonmesomorphic epoxy resin. *J. Polym. Sci., Part A: Polym. Chem.* **2004**, *42*, 3631-3643, <https://doi.org/10.1002/pola.20254>.
 25. Sadagopan, K.; Ratna, D.; Samui, A.B. Synthesis and characterization of liquid-crystalline epoxy and its blend with conventional epoxy. *J. Polym. Sci., Part A: Polym. Chem.* **2003**, *41*, 3375-3383, <https://doi.org/10.1002/pola.10923>.
 26. Chruściel, J.J.; Leśniak, E. Modification of epoxy resins with functional silanes, polysiloxanes, silsesquioxanes, silica and silicates. *Prog. Polym. Sci.* **2015**, *41*, 67-121, <https://doi.org/10.1016/j.progpolymsci.2014.08.001>.
 27. Grich, M.; El Gouri, M.; Ziraoui, R.; Rami, N.; Meghraoui, H.; Cherkaoui, O.; El Harfi, A. Thermal and rheological study of blended carbon nanotube/epoxy resin nanocomposites. *J. Mater. Environ. Sci* **2014**, *5*, 374-379.
 28. Chen, M.; Liang, X.; Hu, W.; Zhang, L.; Zhou, L.; Zhang, C.; Wang, J.; Meng, C.; Fang, J.; Yang, H. Precipitation polymerization in liquid crystals to prepare uniform epoxy microspheres. *Polymer* **2018**, *154*, 291-297, <https://doi.org/10.1016/j.polymer.2018.09.006>.

29. Hsissou, R.; Benzidia, B.; Hajjaji, N.; Elharfi, A. Elaboration and electrochemical studies of the coating behavior of a new nanofunctional epoxy polymer on E24 steel in 3.5% NaCl. *Portugaliae Electrochimica Acta* **2018**, *36*, 259-270, <http://dx.doi.org/10.4152/pea.201804259>.
30. Mahadeva Raju, G.K.; Madhu, G.M.; Ameen Khan, M.; Dinesh Sankar Reddy, P. Characterizing and Modeling of Mechanical Properties of Epoxy Polymer Composites Reinforced with Fly ash. *Materials Today: Proceedings* **2018**, *5*, 27998-28007, <https://doi.org/10.1016/j.matpr.2018.10.040>.
31. Hsissou, R.; Bekhta, A.; Elharfi, A.; Benzidia, B.; Hajjaji, N. Theoretical and electrochemical studies of the coating behavior of a new epoxy polymer: hexaglycidyl ethylene of methylene dianiline (HGEMDA) on E24 steel in 3.5% NaCl. *Portugaliae Electrochimica Acta* **2018**, *36*, 101-117, <http://dx.doi.org/10.4152/pea.201802101>.
32. Srinivasaraonaik, B.; Singh, L.P.; Sinha, S.; Tyagi, I.; Rawat, A. Studies on the mechanical properties and thermal behavior of microencapsulated eutectic mixture in gypsum composite board for thermal regulation in the buildings. *Journal of Building Engineering* **2020**, *31*, 101400, <https://doi.org/10.1016/j.jobe.2020.101400>.
33. El Gouri, M.; El Bachiri, A.; Hegazi, S.E.; Rafik, M.; El Harfi, A. Thermal degradation of a reactive flame retardant based on cyclotriphosphazene and its blend with DGEBA epoxy resin. *Polym. Degradation Stab.* **2009**, *94*, 2101-2106, <https://doi.org/10.1016/j.polymdegradstab.2009.08.009>.
34. Park, H.; Kim, B.; Choi, J.; Cho, M. Influences of the molecular structures of curing agents on the inelastic-deformation mechanisms in highly-crosslinked epoxy polymers. *Polymer* **2018**, *136*, 128-142, <https://doi.org/10.1016/j.polymer.2017.12.055>.
35. Ren, X.-J.; Dai, Y.-J.; Gou, J.-J.; Tao, W.-Q. Numerical study on thermal contact resistance of 8-harness satin woven pierced composite. *International Journal of Thermal Sciences* **2021**, *159*, 106584, <https://doi.org/10.1016/j.ijthermalsci.2020.106584>.
36. Yang, H.; Cai, F.; Luo, Y.; Ye, X.; Zhang, C.; Wu, S. The interphase and thermal conductivity of graphene oxide/butadiene-styrene-vinyl pyridine rubber composites: A combined molecular simulation and experimental study. *Composites Sci. Technol.* **2020**, *188*, 107971, <https://doi.org/10.1016/j.compscitech.2019.107971>.
37. Chen, J.; Liu, B.; Gao, X. Thermal properties of graphene-based polymer composite materials: A molecular dynamics study. *Results in Physics* **2020**, *16*, 102974, <https://doi.org/10.1016/j.rinp.2020.102974>.
38. Tripathy, S.; Jali, P.; Parida, C.; Pradhan, C. Study on biodegradability and thermal behaviour of composites using poly lactic acid and gamma-irradiated fibres of *Luffa cylindrica*. *Chemosphere* **2020**, *261*, 127684, <https://doi.org/10.1016/j.chemosphere.2020.127684>.
39. Ziraoui, R.; Grich, M.; Meghraoui, H.; Elgouri, M.; Mouada, A.; Fetouaki, S.; Elharfi, A. Study of thermal, mechanical and dielectrical properties of a composite material based on DGEBA flexibilized by CTBN. in *Ann. Chim. Sci. Mat.* **2010**, *35*, 99-112.
40. Hsissou, R.; Berradi, M.; El Bouchti, M.; El Bachiri, A.; El Harfi, A. Synthesis characterization rheological and morphological study of a new epoxy resin pentaglycidyl ether pentaphenoxy of phosphorus and their composite (PGEPPP/MDA/PN). *Polym. Bull.* **2019**, *76*, 4859-4878, <https://doi.org/10.1007/s00289-018-2639-9>.
41. Hsissou, R.; Abbout, S.; Safi, Z.; Benhiba, F.; Wazzan, N.; Guo, L.; Nouneh, K.; Briche, S.; Erramli, H.; Ebn Touhami, M.; Assouag, M.; Elharfi, A. Synthesis and anticorrosive properties of epoxy polymer for CS in [1 M] HCl solution: Electrochemical, AFM, DFT and MD simulations. *Construction and Building Materials* **2020**, 121454, [doi:https://doi.org/10.1016/j.conbuildmat.2020.121454](https://doi.org/10.1016/j.conbuildmat.2020.121454).
42. Nayak, R.K.; Ray, B.C. Influence of seawater absorption on retention of mechanical properties of nano-TiO₂ embedded glass fiber reinforced epoxy polymer matrix composites. *Archives of Civil and Mechanical Engineering* **2018**, *18*, 1597-1607, <https://doi.org/10.1016/j.acme.2018.07.002>.
43. Hsissou, R.; Benzidia, B.; Hajjaji, N.; Elharfi, A. Elaboration and electrochemical studies of the coating behavior of a new pentafunctional epoxy polymer (pentaglycidyl ether pentabisphenol phosphorus) on E24 carbon steel in 3.5 % NaCl. *Journal of Chemical Technology and Metallurgy* **2018**, *53*, 898-905.
44. Hsissou, R.; El Bouchti, M.; Elharfi, A. Elaboration and viscosimetric, viscoelastic and rheological studies of a new hexafunctional polyepoxide polymer: Hexaglycidyl Ethylene of Methylene Dianiline. *J. Mater. Environ. Sci* **2017**, *8*, 4349-4361.
45. Hsissou, R.; Bekhta, A.; Elharfi, A. Viscosimetric and rheological studies of a new trifunctional epoxy pre-polymer with noyan ethylene: Triglycidyl Ether of Ethylene of Bisphenol A (TGEEBA). *J. Mater. Environ. Sci* **2017**, *8*, 603-610.

46. Metalwala, Z.; Khoshroo, K.; Rasoulianboroujeni, M.; Tahriri, M.; Johnson, A.; Baeten, J.; Fahimipour, F.; Ibrahim, M.; Tayebi, L. Rheological properties of contemporary nanohybrid dental resin composites: The influence of preheating. *Polym. Test.* **2018**, *72*, 157-163, <https://doi.org/10.1016/j.polymertesting.2018.10.013>.
47. Hsissou, R.; Elharfi, A. Rheological behavior of three polymers and their hybrid composites (TGEEBA/MDA/PN), (HGEMDA/MDA/PN) and (NGHPBAE/MDA/PN). *Journal of King Saud University - Science* **2020**, *32*, 235-244, <https://doi.org/10.1016/j.jksus.2018.04.030>.
48. Zhang, Y.; Cui, L.; Xu, H.; Feng, X.; Wang, B.; Pukánszky, B.; Mao, Z.; Sui, X. Poly(lactic acid)/cellulose nanocrystal composites via the Pickering emulsion approach: Rheological, thermal and mechanical properties. *Int. J. Biol. Macromol.* **2019**, *137*, 197-204, <https://doi.org/10.1016/j.ijbiomac.2019.06.204>.
49. Liao, W.; Wang, G.; Liu, Z.; Xu, S.; Wang, Y.-Z. Rheological premonitory of nanoclay morphology on the mechanical characteristics of composite aerogels. *Composites Part B: Engineering* **2019**, *173*, 106889, <https://doi.org/10.1016/j.compositesb.2019.05.100>.
50. Liu, R.; Wang, X. Synthesis, characterization, thermal properties and flame retardancy of a novel nonflammable phosphazene-based epoxy resin. *Polym. Degradation Stab.* **2009**, *94*, 617-624, <https://doi.org/10.1016/j.polymdegradstab.2009.01.008>.
51. Lee, K.-H.; Bae, J.-S.; Yeum, J.H.; Park, J.; Sung, C.; Kim, J.; Oh, W. Thermal characteristics of epoxy composites with graphite and alumina. *Thermochim. Acta* **2019**, *676*, 115-119, <https://doi.org/10.1016/j.tca.2019.04.004>.
52. Hou, M.; Kong, X.; Li, H.; Yang, H.; Chen, W. Experimental study on the thermal performance of composite phase change ventilated roof. *Journal of Energy Storage* **2020**, 102060, <https://doi.org/10.1016/j.est.2020.102060>.
53. Kumar, E.A.; Jivraj, K.B.; Babu, K.S. Study of ammonia adsorption/desorption characteristics of CaCl₂ – Expanded natural graphite composite for thermal energy storage. *Thermal Science and Engineering Progress* **2020**, *20*, 100752, <https://doi.org/10.1016/j.tsep.2020.100752>.
54. Melánová, K.; Beneš, L.; Zima, V.; Trchová, M.; Stejskal, J. Polyaniline–zirconium phosphonate composites: Thermal stability and spectroscopic study. *J. Phys. Chem. Solids* **2020**, *147*, 109634, <https://doi.org/10.1016/j.jpcs.2020.109634>.
55. Xu, C.; Miao, M.; Jiang, X.; Wang, X. Thermal conductive composites reinforced via advanced boron nitride nanomaterials. *Composites Communications* **2018**, *10*, 103-109, <https://doi.org/10.1016/j.coco.2018.08.002>.
56. Pan, J.; Bian, L. A physics investigation for influence of carbon nanotube agglomeration on thermal properties of composites. *Mater. Chem. Phys.* **2019**, *236*, 121777, <https://doi.org/10.1016/j.matchemphys.2019.121777>.
57. Saravanan, A.K.; Rajendra Prasad, A.; Muruganandam, D.; Saravanan, G.; Vivekanandan, S.; Sudhakar, M. Study on natural fiber composites of jute, pine apple and banana compositions percentage of weight basis for thermal resistance and thermal conductivity. *Materials Today: Proceedings* **2020**, <https://doi.org/10.1016/j.matpr.2020.04.662>.
58. Wang, J.; Chen, Y.; Feng, Y.; Zhao, G.; Jian, X.; Huang, Q.; Yang, L.; Xu, J. Influence of porosity on anisotropic thermal conductivity of SiC fiber reinforced SiC matrix composite: A microscopic modeling study. *Ceram. Int.* **2020**, *46*, 28693-28700, <https://doi.org/10.1016/j.ceramint.2020.08.029>.
59. Im, D.S.; Hong, B.M.; Kim, M.H.; Park, W.H. Formation of human hair-Ag nanoparticle composites via thermal and photo-reduction: A comparison study. *Colloids Surf. Physicochem. Eng. Aspects* **2020**, *600*, 124995, <https://doi.org/10.1016/j.colsurfa.2020.124995>.